Parametric Effects of Helical Coil Heat Exchanger Design on Thermal-Hydraulic Performance of Passive Molten Salt Fast Reactor

Seungmin Lee [a], Dowon Lee [a], Juhyeong Lee [a], Sung Joong Kim [a, b*]
[a]*Department of Nuclear Engineering, Hanyang University, 222 Wangsimni-ro, Seongdong-gu, Seoul 04763, Republic of Korea*
[b]*Institute of Nano Science & Technology, Hanyang University, 222 Wangsimni-ro, Seongdong-gu, Seoul 04763 Republic of Korea*
**Corresponding author: sungjkim@hanyang.ac.kr*

Keywords : Passive Molten salt Fast Reactor (PMFR); helical coil heat exchanger; thermal-hydraulic performance; sensitivity analysis; natural circulation

1. Introduction

Pursuing low-carbon energy sources has increased interest in deployment of nuclear energy in various energy sectors. Among various nuclear reactor technologies, Molten Salt Reactor (MSR) has been proposed as a promising concept owing to improved passive safety by adopting liquid fuel system as well as its applicability into the broad energy sectors by high temperature operation. The liquid fuel is expected to increase the inherent safety features and efficient fuel utilization. However, the research and development of MSRs at current stage confront significant challenges due to possible corrosion by salt matrix and thermal stress under high temperature operation. These challenges have been reported and significant research efforts are underway to resolve. As well, since 2021 a research consortium teamed by Hanyang University, KAIST, and Gachon University initiated a development of conceptual MSR called Passive Molten salt Fast Reactor (PMFR), with which various fundamental MSR technologies are under development [1].

Unlike most traditional MSRs relying on pumps or active safety systems, the PMFR has been designed to operate by natural circulation and to employ a helical type heat exchanger (HX). Such design concept enables to eliminate or reduce the dependence on active components, to simplify the reactor system, and finally to enhance safety and sustainability substantially. The key feature of the PMFR is to maintain coolant flow without operator intervention, which makes the PMFR concept more distinguishable relative to the earlier MSR concept.

In advancing the PMFR concept to the system level, the performance of the HX bridging the primary and secondary systems via natural circulation loop plays a crucial role in determining the fuel salt temperature, which directly affects the flow rate and overall safety. In addition, because the liquid fuel salt functions as the coolant and fuel in a homogenous matrix, the primary-side HX volume becomes a decisive factor in determining the fuel salt inventory. Note that because the current concept of PMFR excludes any active pumps and relies on natural circulation, overall dimension of the reactor could be larger relative to the pumped system, otherwise securing sufficient thermal center to drive power-scoping natural circulation performance will be infeasible. Therefore, minimizing the total amount of primary-side fuel salt becomes a critical task to delineate the realistic fuel inventory for this concept. In the perspective of thermal-performance of the PMFR, a HX design proposed should be able to accommodate the target power output, which is the major topic in this study.

Thus, this study aims to assess the feasibility of the PMFR by exploring various HX design parameters to minimize its volume. A one-dimensional model of the PMFR was developed and several key geometric parameters of the helical coil type HX, such as the number of transversal and longitudinal tube rows and the helical coil diameter, were investigated. Impact of these parameters on the critical variables including the fuel salt temperature and the secondary loop pressure was then analyzed. To reflect the PMFR's power distribution and to assess its natural circulation performance, a GAMMA+ input model was developed and used throughout this study.

2. Numerical Methodology

2.1 Concept of Passive Molten salt Fast Reactor

As shown in **Figure 1**, the Passive Molten salt Fast Reactor (PMFR) consists of a riser, active core, upper plenum, helical coil heat exchanger (HX), downcomer, and lower plenum [2]. To operate the PMFR by natural circulation, the primary system is designed as a long cylinder of 15 m, in which a helical type HX is introduced. In the active core region, the liquid fuel salt generates the heat through the fission and induces the flow by buoyancy force. The flow rises through a long riser and reaches the upper plenum. The heated fuel salt is circulated through HX region and cooled by the secondary coolant non-fueled salt. While repeating this cycle, the cooled salt is circulated back into the active core region via the downcomer.

To ensure the solubility of uranium fuel and decrease the melting temperature of fuel salt, the PMFR adopts a ternary fuel salt matrix, which consists of NaCl-KCl-UCl3. The target power of PMFR ranges 200 to 300 MWt, and target primary fuel salt temperature ranges

500~650 °C. The major design parameters of the PMFR are presented in **Table 1**.

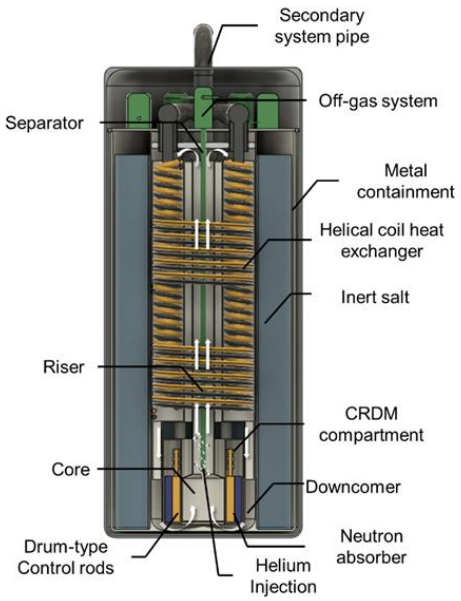

Fig. 1 Schematic diagram of PMFR system

Table 1: Design parameters of PMFR

Parameter	Description
Reactor thermal output	200 MWt
Plant design life	20~40 years
Fuel salt	NaCl-KCl-UCl3
Reactor height	15 m
Heat exchanger type	Helical coil
Reactor Core	H: 1.95 m, D: 2 m
Riser	H: 13.05 m, D: 0.6 m

2.2 GAMMA+ input model

GAMMA+ is the system code, which was developed by Korea Atomic Energy Research Institute with primary target for simulating GEN-IV reactors. GAMMA+ provides the thermophysical properties of fuel salt, coolant salt, and numerous models for HXs. To simulate the natural circulation behavior of PMFR, the GAMMA+ input model was constructed based on the basic design information summarized in **Table 1**.

The initial conditions were set based on steady-state operating condition, with a primary loop HX initial inlet temperature of 735°C and the initial outlet temperature of 551°C. The flow rate of the secondary loop was fixed to 1500kg/s.

Figure 2 shows the nodal information of PMFR. From the top, the fuel salt flows sequentially through the upper plenum, HX, downcomer, lower plenum, core, and riser. The core consists of five channels, allowing for the consideration of radial temperature variations. The lengths of the HX and downcomer are dependent on the number of longitudinal tube rows. As the longitudinal tube rows increase, the HX length increases while the downcomer length decreases accordingly. The secondary-side HX maintains the same length as the primary-side HX and is connected to the inlet and outlet boundary conditions. The HX was discretized into five nodes based on a nodal sensitivity analysis conducted with 5, 10, 15, and 20 nodes. The relative errors in inlet temperature were 0.087%, 0.030%, and 0.013%, while those in outlet temperature were 0.026%, 0.008%, and 0.004%, respectively. As the differences were minimal, the five-node configuration was adopted to balance accuracy and computational efficiency.

The wall block is discretized into five axial and four radial meshes, facilitating the heat transfer calculation between the primary and secondary heat exchangers.

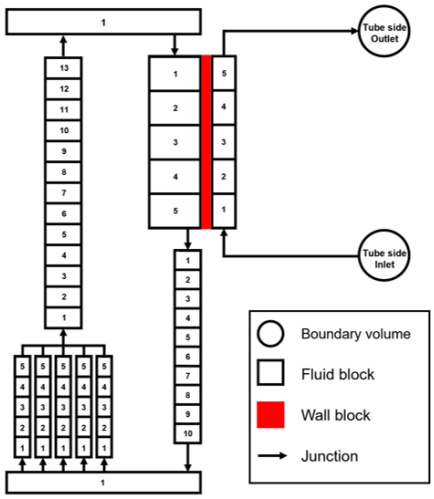

Fig. 2 nodal information of PMFR

In the PMFR system, major contributors of the pressure drop could be sudden expansion, sudden contraction, and geometrical values of HX. Among these, the pressure drop from sudden expansion and contraction were calculated by Eqs. (1) and (2), which were incorporated into the input.

For sudden expansion [3],

$$K_{SE} = \left(1 - \frac{d^2}{D^2}\right)^2 \quad (1)$$

For sudden contraction [3],

$$K_{SC} = 1.41e^{-0.48\left(\frac{A_2}{A_1}\right)} - 0.89 \quad (2)$$

2.3 Heat exchanger model and sensitivity parameters

As depicted in **Figure 3**, the helical coil HX consists of thin tubes, through which the secondary loop's coolant salt flows. These tubes are arranged in an annular shell side, where the primary loop's fuel salt flows downward between the tubes. A counterflow configuration is established by having the secondary coolant salt flow upward, thus maintaining a constant temperature difference between the two fluids and improving heat

transfer efficiency.

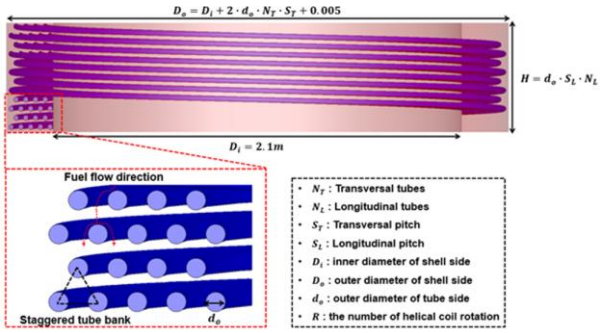

Fig. 3 Schematic diagram of helical coil HX system

In this study, a triangular helical coil configuration is employed for the HX, whose configuration is an equilateral triangle, leading to a transversal pitch-to-diameter ratio (P/D) of 2 and a longitudinal P/D of √3.

The HX inner diameter (D_i) was fixed at 2.1 m, slightly larger than the core diameter of 2 m, while the outer diameter (D_o) was adjusted based on the number of transversal tube rows. To prevent overlapping with the core, the HX length was set to be less than 13.05 m, corresponding to the riser height.

As shown in Eq. (3), the number of transversal tube rows exhibit a greater impact on the overall volume than the longitudinal tube rows because when the equations related to the number of rows are substituted into the volume equation, the transversal tube rows become a quadratic term, while the longitudinal tube rows remain a linear term. In addition, as observed in **Figure 4**, an increase in transversal tube rows results in a reduction of the heat transfer area for a given volume. Thus, to minimize the volume of the HX, the number of transversal tube rows was minimized, which, in turn, resulted in the number of longitudinal tube rows being increased as much as possible within the design constraints.

$$V = \frac{({D_o}^2 - {D_i}^2)\pi L}{4} \tag{3}$$

where D_o is the HX outer diameter, D_i is the HX inner diameter, and L is the length of the HX.

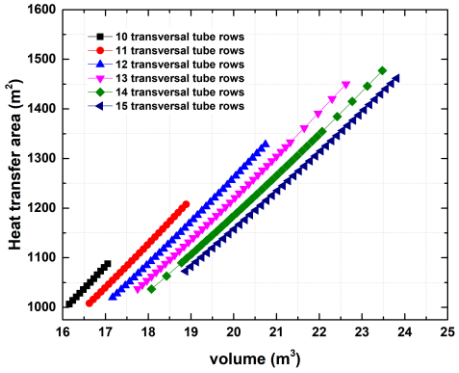

Fig. 4 Heat transfer area as a function of volume for different transversal tube rows

Heat transfer and pressure drop of helical tube shell side and tube side are calculated respectively using the models supported by GAMMA+, as represented by Eqs. (4), (5), (6), (7), (8), and (9). These correlations enable performance evaluation of the PMFR's heat exchanger by predicting thermal and hydraulic behavior across different mass flow rates, tube diameters, and coil geometries.

For tube side heat transfer [4],

$$Nu \cdot Pr^{-0.4} = \frac{1}{41.0} Re^{\frac{5}{6}} \left(\frac{d_{tube}}{D_{coil}}\right)^{\frac{1}{12}} \left[1 + \frac{0.061}{\left\{Re\left(\frac{d_{tube}}{D_{coil}}\right)^{2.5}\right\}^{\frac{1}{6}}}\right] \tag{4}$$

provided that Pr>1, where d_{tube} is the tube diameter and D_{coil} is average of diameter of coil.

For tube side pressure drop [4],

$$\Delta P = f \frac{L}{D_{coil}} \frac{1}{2} \rho {v_c}^2 \tag{5}$$

$$f = \left(\frac{d_{tube}}{D_{coil}}\right)^{0.5} \frac{0.192}{\left[Re\left({}^{d_{tube}}/_{D_{coil}}\right)^{2.5}\right]^{\frac{1}{6}}} \times \left\{1 + \frac{0.068}{\left[Re\left({}^{d_{tube}}/_{D_{coil}}\right)^{2.5}\right]^{\frac{1}{6}}}\right\} \tag{6}$$

where v_c is velocity in the tube fluid, d_{tube} is inner diameter of tube and D_{coil} is average diameter of coil.

For shell side heat transfer [5],

$$Nu = 0.35 \left(\frac{a}{b}\right)^{0.2} {Re_f}^{0.60} {Pr_f}^{0.36} \left(\frac{Pr_f}{Pr_w}\right)^{0.25} \tag{7}$$

where a is transversal P/D and b is longitudinal P/D.

For shell side pressure drop [5],

$$\Delta P = Eu \cdot \frac{1}{2} \rho {v_m}^2 \cdot N \tag{8}$$

where v_m is velocity of fuel salt and N is the number of tube arrays.

$$\frac{Eu}{k_1} = 0.162 + \frac{0.181 \times 10^4}{Re} + \frac{0.792 \times 10^8}{Re^2} - \frac{0.165 \times 10^{13}}{Re^3} + \frac{0.872 \times 10^{16}}{Re^4} \tag{9}$$

where helical tube configuration is an equilateral triangular array, $k_1 = 1$

2.4 Heat exchanger design parameters

To investigate the effect of different geometric parameters on the thermal-hydraulic performance of the PMFR, the secondary loop pressure and fuel salt temperature were evaluated for three representative tube diameters. The secondary loop pressure drop was maintained below 2 MPa to minimize material fatigue and corrosion risks, as higher pressures impose greater stress on the piping and heat exchanger materials. It was found that for tube diameters smaller than 9 mm, the secondary loop pressure constraint was not satisfied. Therefore, three cases with tube diameters of 9 mm, 11 mm, and 13 mm were investigated. However, the limitation of the secondary loop pressure drop to 2 MPa was arbitrarily set during the preliminary analysis. This value is subject to refinement in future studies based on more detailed assessments.

In case of the smallest diameter (9 mm), the small tube size resulted in a higher pressure drop. When the number of helical coil rotations was set to two, the target secondary pressure could not be satisfied; therefore, only one coil rotation was used. For the other two diameters (11 mm and 13 mm), the number of helical coil rotations was maintained at two.

Table 2 summarizes the key design parameters such as tube diameter and number of coil rotations, along with the resulting secondary loop pressure range and required HX volume range, under the constraint that the maximum fuel salt temperature stays close to 650°C.

Table 2: Comparison of different helical coil design cases

Cases	Tube Diameter (mm)	Number of Helical Tube Rotation	Secondary Loop Pressure (MPa)	HX Volume Range (m^3)
Case 1	9	1	0.6366–1.0253	16.24–21.91
Case 2	11	2	1.2678–1.9855	16.73–22.31
Case 3	13	2	0.6542–1.0313	21.58–29.93

3. Result

In **Table 2**, the pressure range of Case 2 is 1.27–1.99 MPa, remaining below the 2 MPa target limit. In Case 3, the pressure range is 0.65–1.03 MPa, indicating a relatively lower pressure drop compared to Case 2. However, the larger tube diameter in Case 3 leads to an increased HX volume requirement. For Case 1 (smallest diameter), the pressure drop is even higher if two coil rotations are attempted, hence only one rotation could achieve the secondary loop pressure lower than that of case 2.

Figures 5, 6, and **7** illustrate the influence of HX volume and the number of transversal tube rows on the maximum fuel salt temperature. In all cases, increasing the HX volume decreases the maximum temperature of primary system. This behavior is consistent over the three diameters, indicating that a larger heat transfer area and fluid capacity enhance the overall cooling effect. However, a lower number of transversal tube rows consistently decreases maximum temperature for a given volume. Increasing the number of transversal tube rows leads to a situation where the volume of the heat exchanger grows faster than the increase in heat transfer area. Consequently, the amount of heat exchanged per unit volume actually decreases. The results show that simply increasing the number of tube rows may not always be an effective strategy for improving thermal performance.

The slope of the graph represents the rate of decrease in the maximum fuel salt temperature as the heat exchanger volume increases. A larger absolute value of the slope indicates that the fuel salt temperature drops more rapidly with a small volume increase, meaning that effective cooling can be achieved with a relatively smaller heat exchanger. Consequently, the target temperature can be met with minimizing the overall system size.

As shown in **Figures 5, 6,** and **7**, the fuel salt temperature decreases by an average of 3.39°C, 2.92°C, and 2.39°C per cubic meter of heat exchanger volume, respectively. This trend is clearly illustrated in **Figure 8**, which presents representative data points that effectively capture the average slope for each tube diameter. For the 9 mm case, the value corresponding to 11 transversal tube rows was used, while for the 11 mm and 13 mm cases, data from 10 transversal tube rows were utilized. This difference can lead to a significant impact when considering a heat exchanger with a volume of approximately 20 m³. A comparison of **Figures 6** and **7**, which correspond to Case 2 and Case 3, reveals that to achieve a maximum fuel salt temperature of 650°C the required heat exchanger volume in Case 3 is 31.4% larger than that in Case 2 despite both cases utilizing two helical coil turns.

As a result, while larger tube diameters can improve flow characteristics and potentially reduce pressure drop, they also require a larger HX volume to reach comparable temperature reductions as seen in smaller-diameter configurations. Therefore, selecting an appropriate tube diameter must account for both thermal performance and geometric constraints.

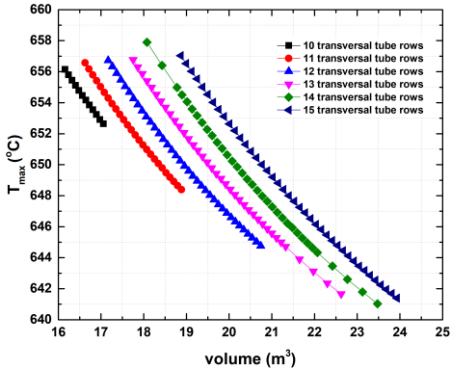

Fig. 5 Fuel salt maximum temperature as a function of volume for case 1

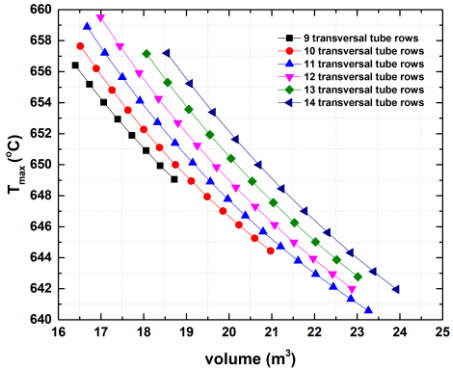

Fig. 6 Fuel salt maximum temperature as a function of volume for case 2

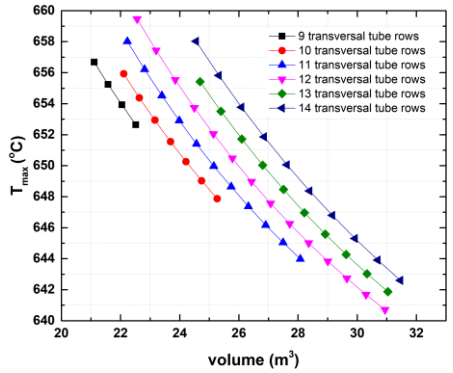

Fig. 7 Fuel salt maximum temperature as a function of volume for case 3

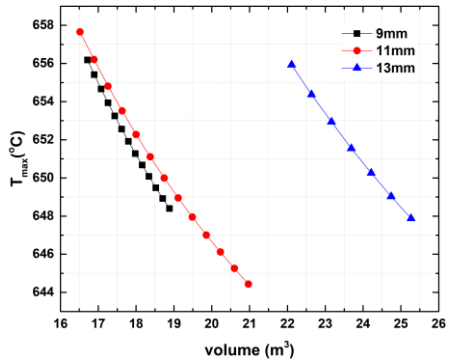

Fig. 8 Fuel salt maximum temperature as a function of volume for different tube diameters

4. Summary and Conclusion

In this study, we highlight the impact of key design parameters in the helical coil HX, such as tube diameter, number of coil rotations, and transversal/longitudinal tube rows, on the natural circulation performance of the PMFR by using the GAMMA+ code. The results show the importance of appropriately balancing HX volume, tube diameter, and the number of transversal tube rows to achieve an optimal design. Future studies are planned to refine the observed findings by examining additional geometric variations, operational conditions, and economic considerations to guide more comprehensive design recommendations.

ACKNOWLEDGMENTS

This research was supported by the National Research Foundation of Korea (NRF) and funded by the ministry of Science, ICT, and Future Planning, Republic of Korea (grant numbers RS-2021-NR056168), and the Human Resources Development of the Korea Institute of Energy Technology Evaluation and Planning (KETEP) grant funded by the Korea government Ministry of Knowledge Economy (RS-2024-00439210).

REFERENCES

[1] J. H. Park, W. J. Choi, J. H. Lim, T. S. Kim, Y. H. Kim, Y. S. Yoon, S.T. Kim and S. J. Kim, Design Concepts and Requirements of Passive Molten Salt Fast Reactor (PMFR), Transactions of the Korean Nuclear Society Spring Meeting Jeju, Korea, 2022.
[2] J. H. Im, J. H. Park, W. J. choi and S. J. Kim, Preliminary Design of System-integrated Heat Exchangers for Passive Molten Salt Fast Reactor, Transactions of the Korean Nuclear Society Spring Meeting, 2024
[3] F. M. White, Fluid Mechanics, McGraw and Hill, New York, 7th edn, 2011.
[4] Y. Mori and W. Nakayama, Study on Forced Convective Heat Transfer in Curved Pipes, Int. J. Heat Mass Transfer, Vol. 10, pp. 37-59, 1967.
[5] J. P. Hartnett, Advanced in Heat Transfer, Academic Press, New York, Vol.8, 1972.
[6] E. U. Schlunder, Heat exchanger design handbook, Hemispere Publishing Corporation, USA, 1983.